Regulation of Clock and NPAS2 DNA Binding by the Redox State of NAD Cofactors

Jared Rutter,* Martin Reick,* Leeju C. Wu, Steven L. McKnight†

Clock:BMAL1 and NPAS2:BMAL1 are heterodimeric transcription factors that control gene expression as a function of the light-dark cycle. Although built to fluctuate at or near a 24-hour cycle, the clock can be entrained by light, activity, or food. Here we show that the DNA-binding activity of the Clock:BMAL1 and NPAS2:BMAL1 heterodimers is regulated by the redox state of nicotinamide adenine dinucleotide (NAD) cofactors in a purified system. The reduced forms of the redox cofactors, NAD(H) and NADP(H), strongly enhance DNA binding of the Clock:BMAL1 and NPAS2:BMAL1 heterodimers, whereas the oxidized forms inhibit. These observations raise the possibility that food, neuronal activity, or both may entrain the circadian clock by direct modulation of cellular redox state.

In organisms as diverse as fruit flies and mammals, circadian rhythms are controlled by a transcriptional feedback system whose activity fluctuates as a function of the light-dark (LD) cycle (*1*, *2*). In mammals, the positive arm of this system is specified by a heterodimeric transcription factor composed of the products of the *Clock* and *BMAL1* genes (*3*). The mammalian *NPAS2* gene encodes a functional analog of Clock (*4*, *5*) but is expressed in a distinct pattern of tissues including the prefrontal cortex of the brain.

The Clock:BMAL1 and NPAS2:BMAL1 heterodimers regulate the expression of genes encoding other components of the molecular clock. Both complexes activate expression of the *Per2* and *Cry1* genes, which themselves encode negative components of the clock (*4*, *6*, *7*). In addition, the NPAS2:BMAL1 heterodimer represses *BMAL1* gene expression (*4*). Because BMAL1 is an obligate component of the activating arm of the rhythmic oscillator and BMAL1 mRNA levels fluctuate rhythmically as a function of the LD cycle (*4*, *8*), the repressive action of NPAS2:BMAL1 on *BMAL1* gene expression ensures that the clock oscillates in a faithful and robust manner.

In the absence of environmental influences, the circadian regulatory apparatus oscillates at or close to the 24-hour LD cycle. Extrinsic factors including light, temperature, activity, and food can advance or delay the system, thereby synchronizing the intrinsic clock with the external environment (*9*, *10*). This coupling of environmental cues to the intrinsic clock is termed entrainment. Extensive studies have demonstrated that light entrains the intrinsic clock by a pathway linking the retina to the suprachiasmatic nucleus (SCN), the site of the master circadian pacemaker (*11*). Food is also capable of entraining behavioral rhythms driven by the circadian clock. For example, circadian locomotor activity can be entrained by restricted feeding (RF) of rodents independent of the LD cycle (*12*, *13*). This entrainment of behavioral rhythms is accompanied by a concordant change in the molecular clock in most tissues (*14*–*16*). Here we present biochemical data that suggest a simple mechanism by which activity or food ingestion may entrain the circadian regulatory apparatus.

In the accompanying report (*4*), we developed a human neuroblastoma cell culture system to identify putative target genes of the NPAS2:BMAL1 heterodimer. The gene encoding the A isoform of lactate dehydrogenase (LDHA) was one of about 90 genes activated by induction of this transcription factor. Northern blot assays (*17*) confirmed that the neuroblastoma cells rapidly accumulated high levels of LDHA mRNA upon induction of NPAS2:BMAL1 (Fig. 1, inset). We prepared a construct in which a luciferase reporter gene was placed under the control of the human LDHA promoter. Expression from this LDHA-luciferase reporter was markedly induced in cultured 293 cells upon cotransfection of expression vectors encoding NPAS2 and BMAL1 (Fig. 1) (*4*, *18*). These observations suggest that LDHA is a direct and bona fide transcriptional target of NPAS2:BMAL1. Three additional findings support this interpretation: (i) the LDHA promoter contains two optimal NPAS2:BMAL1 binding sites (*19*), (ii) the NPAS2:BMAL1–dependent increase in LDHA levels was attenuated by CRY1, a repressor of CLOCK and NPAS2 transcriptional activity (Fig. 1), and (iii) the basal level of LDHA-driven luciferase activity was also attenuated by CRY1. Endogenous, CRY1-repressible NPAS2:BMAL1 activity, therefore, may contribute substantially to the basal level of LDHA-luciferase expression.

LDHA reversibly catalyzes the enzymatic conversion of pyruvate to lactate (*20*). In the forward direction, the reaction consumes reduced nicotinamide adenine dinucleotide (NADH) and evolves balanced levels of the oxidized form of the cofactor (NAD). Knowing that the redox state of NAD(H) might change as a function of LDHA expression or rhythmic food intake, we reasoned that these cofactors could be part of a feedback mechanism controlling the molecular clock. We therefore tested the possibility that the redox state of either NAD(H) or NADP(H) might directly control the activity of the NPAS2:BMAL1 transcription factor.

We first tested this hypothesis by monitoring the DNA-binding activity of NPAS2:BMAL1 in vitro by an electrophoretic mobility shift (EMS) assay (*21*, *22*). This assay revealed two species of DNA-binding activity, one corresponding to NPAS2:BMAL1 and the other corresponding to the BMAL1:BMAL1 homodimer. Both NADH and NADPH induced the DNA-binding activity of NPAS2:BMAL1 (Fig. 2). Half-maximal induction (EC_{50}) was observed at concentrations of 6.3 mM NADH and 2.3 mM NADPH, both of which are within physiological ranges (*23*). By contrast, NADH and NADPH did not stimulate the DNA-binding activity of BMAL1:BMAL1 but rather appeared to attenuate it. Because the NAD cofactors do not affect BMAL1:BMAL1 DNA binding in the absence of NPAS2 (see below), we speculate that NADH and NADPH inhibit BMAL1:BMAL1 DNA-binding activity by favoring the incorporation of BMAL1 into the NPAS2:BMAL1 heterodimer.

It is unlikely that the absolute levels of NAD cofactors fluctuate as a function of the LD cycle, food ingestion, or neuronal activity. We therefore performed a more physiologically relevant experiment in which we left the total NAD(H) or NADP(H) level constant but altered the ratios of the reduced and oxidized forms of these cofactors. These experiments revealed that the DNA-binding activity of NPAS2:BMAL1 was optimal when the ratio of reduced-to-oxidized NADP(H) cofactor exceeded 75% (Fig. 3A). Above this ratio, DNA binding increased steeply, whereas below this ratio it was acutely diminished. We saw similar results when we altered the ratios of NAD(H) rather than NADP(H) (*24*).

When applied in the absence of balancing levels of their oxidized counterparts, NADH and NADPH induced NPAS2:BMAL1 DNA binding with respective EC_{50}'s of 6.3 mM and 2.3 mM (Fig. 2). When tested in balanced

Department of Biochemistry, University of Texas–Southwestern Medical Center, 5323 Harry Hines Boulevard, Dallas, Texas 75390–9152, USA.

*These authors contributed equally to this work.
†To whom correspondence should be addressed. E-mail: smckni@biochem.swmed.edu

mixes, the EC_{50}'s for NADH and NADPH increased to 9.0 mM and 4.1 mM, respectively (Fig. 3A). The discrepancy between these EC_{50} values raised the possibility that the oxidized forms of the two cofactors might inhibit NPAS2:BMAL1 DNA-binding activity. To test this, we performed a titration experiment in which the NPAS2:BMAL1 heterodimer, supplemented with NADPH at 2.0 mM, was challenged with graded increases of the oxidized form of the cofactor (NADP). As shown in Fig. 3B, NADP inhibited NPAS2:BMAL1 DNA binding with a half-maximal inhibition (IC_{50}) at a concentration of 0.56 mM. NAD titration inhibits NADH-induced NPAS2:BMAL1 DNA binding similarly to NADP (*24*).

The inhibitory effect of NADP may account for the unusually steep induction curve observed in the ratio experiment (Fig. 3A). Quantitation of NPAS2:BMAL1 DNA-binding activity in this experiment revealed a 9.3-fold increase between the 60:40 and 80:20 reduced-to-oxidized cofactor ratios, generating an induction curve with a Hill coefficient of 15. The reactions programmed with the 60:40 and 80:20 ratios contained 3 and 4 mM NADPH, respectively. In the absence of balanced levels of NADP, a similar 9.4-fold change in NPAS2:BMAL1 DNA-binding activity occurred between 1 and 3 mM NADPH (Fig. 2A), corresponding to an induction curve with a Hill coefficient of 3.7. The relatively steeper induction curve observed in the NADP(H) ratio experiment likely reflects the fact that the reduced and oxidized forms of NADP(H) influence NPAS2:BMAL1 DNA-binding activity reciprocally.

We next measured binding constants for NPAS2:BMAL1 as a function of NADP(H) redox state, assessed at an invariant 5 mM NADPH level. We challenged a constant amount of input heterodimer with systematically increased amounts of radioactive DNA substrate, using the EMS assay to separate protein-bound complex from free DNA (*25*). Figure 4 shows saturation binding curves indicative of the DNA-binding properties of NPAS2:BMAL1 measured at NADPH:NADP ratios of 50:50, 60:40, 70:30, 80:20, and 90:10, revealing respective dissociation constants (K_d) of 256, 108, 92, 41, and 39 nM, respectively. The total amount of oligonucleotide bound (B_{max}) varied substantially as a function of redox state, increasing steadily as the ratio of reduced-to-oxidized cofactor was elevated. Over the relative subtle change of 50:50 to 80:20 NADPH:NADP, the affinity (K_d) of NPAS2:BMAL1 for its optimal DNA recognition site increased 6.3-fold and the maximal saturable binding (B_{max}) increased 3.4-fold.

To assess the specificity of this response to NADPH, we compared the effects of NADPH on the DNA-binding activity of NPAS2:BMAL1, Clock:BMAL1, BMAL1:BMAL1, and ARNT1:ARNT1. NADPH enhanced the DNA-binding activity of NPAS2:BMAL1 and Clock:BMAL1 but had no effect on BMAL1:BMAL1 or ARNT1:ARNT1 (Fig. 5). NADPH also had no effect on NPAS2 and Clock in the absence of their obligate heteromeric partner—neither protein alone bound DNA with or without NADPH. Finally, both Clock and NPAS2 were found to bind to the optimal NPAS2:BMAL1 DNA recognition site when mixed with equimolar ratios of ARNT1 rather than BMAL1. Although these heterodimers may not be physiologically relevant, both Clock:ARNT1 and NPAS2:ARNT1 were responsive to NADPH (Fig. 5). In summary, these observations indicate that only NPAS2 and Clock confer responsiveness to NADPH, yet this response is dependent on the presence of either BMAL1 or ARNT1 as a heterodimeric partner.

NPAS2 and Clock are highly related in amino acid sequence (*26*, *27*); their bHLH DNA-binding domains are 84% identical, and their PAS-A and PAS-B domains are 69 and 90% identical, respectively. To define the minimal domain sufficient to confer NADPH responsiveness, we assayed truncated forms of NPAS2 and BMAL1 for DNA-binding

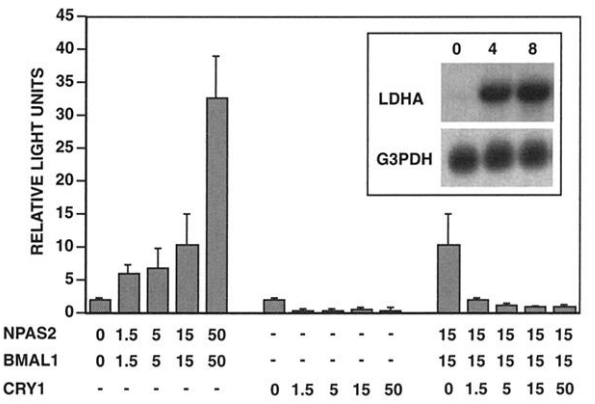

Fig. 1. NPAS2:BMAL1 expression induces accumulation of LDHA mRNA in cultured neuroblastoma cells. Human embryonic kidney 293 cells were cotransfected with the indicated nanogram amounts of expression vectors encoding NPAS2, BMAL1, and CRY1 (*48*), along with a constant amount of a luciferase reporter gene driven by 1.5 kb of 5′ flanking DNA corresponding to the LDHA promoter (*18*). Cells were lysed and assayed for luciferase enzyme activity 20 hours after transfection (*4*). Relative light units are shown ± SD (n = 3). (Inset) SHEP neuroblastoma cells carrying stably transfected, ecdysone-inducible expression plasmids encoding NPAS2 and BMAL1 (*4*) were treated with ponasterone for 4 or 8 hours. LDHA and G3PDH mRNA levels were assayed by Northern blotting (*17*).

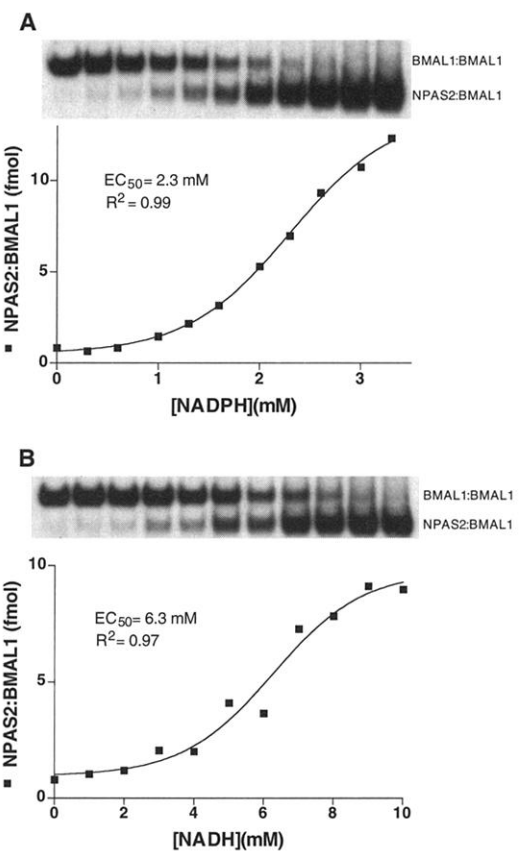

Fig. 2. NADPH and NADH enhance NPAS2:BMAL1 DNA-binding activity in vitro. (**A**) NPAS2 and BMAL1 bHLH-PAS–containing proteins were subjected to EMS DNA-binding assays in the presence of varying amounts of NADPH (*22*). The upper band in the autoradiograph corresponds to DNA-bound BMAL1 homodimer, and the lower band corresponds to DNA-bound NPAS2:BMAL1 heterodimer. The latter was quantitated by phosphorimaging, plotted, and curve fit as shown in the graph, with the corresponding EC_{50} and R^2 values as shown. (**B**) Same as (A), except reactions were incubated with NADH instead of NADPH.

activity in the absence and presence of NAD cofactors. Full responsiveness to NADPH was maintained by the NH_2-terminal 116 amino acids of NPAS2 (Fig. 6). This fragment contained the intact bHLH domain yet lacked both PAS domains. Similarly, a robust response to NADPH was maintained in binding reactions programmed with a minimal bHLH domain of BMAL1 (Fig. 6). As such, reduced forms of nicotinamide-derived cofactors were capable of stimulating DNA binding of the NPAS2:BMAL1 heterodimer through a complex completely devoid of PAS domains (*28*).

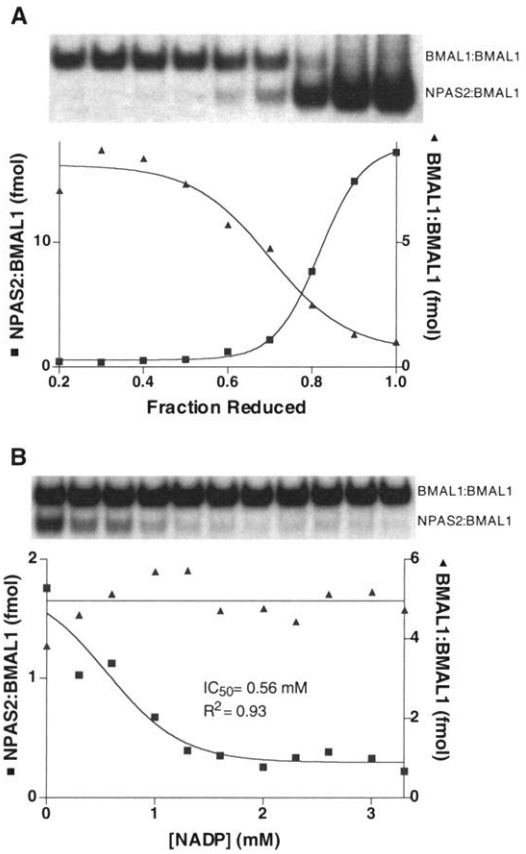

Fig. 3. NADP inhibition creates a highly responsive DNA-binding species. (**A**) NPAS2 and BMAL1 bHLH-PAS–containing proteins were subjected to EMS assays in the presence of varied ratios of NADP and NADPH. The total NADP(H) concentration was held constant at 5 mM, with the mixture being composed of a 20% NADPH:80% NADP molar ratio on the far left to 100% NADPH on the far right and varying in 10% increments for intervening data points as indicated on the *x* axis. (**B**) EMS assays were performed as in Fig. 2, except that the reactions were supplemented with 2 mM NADPH. NADP was added to the reactions at concentrations indicated on the *x* axis. In (A) and (B), the DNA-bound forms of NPAS2:BMAL1 and the BMAL1 homodimer were quantitated by phosphorimaging, plotted, and curve fit (*22*).

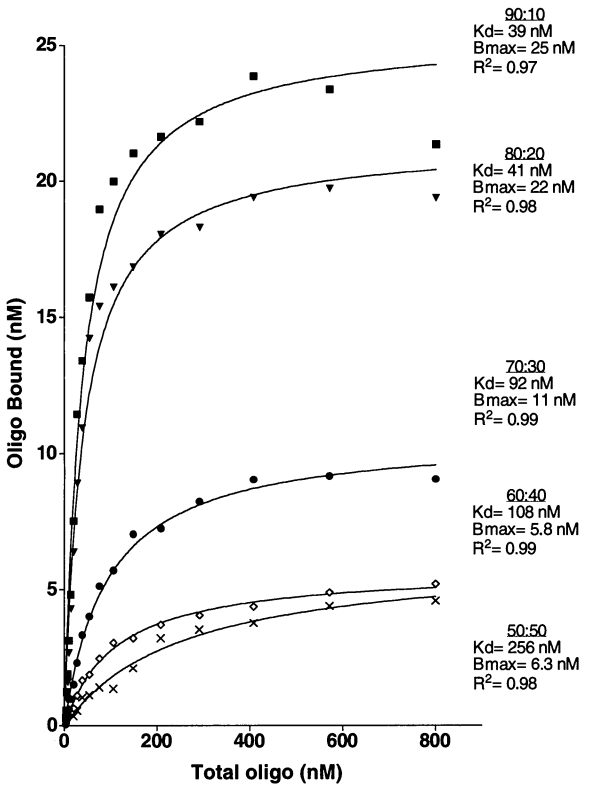

Fig. 4. Saturation plots of NPAS2:BMAL1 DNA binding as a function of NADP(H) redox state. Each saturation plot represents the quantitation of EMS assays with increasing amounts of double-stranded DNA corresponding to the optimal NPAS2:BMAL1 recognition site. Individual experiments were carried out in the presence of varied ratios of NADPH and NADP (90:10, 80:20, 70:30, 60:40, and 50:50), with a constant 5 mM NADP(H) cofactor level. The best-fit curves are shown for each condition, yielding the indicated K_d, B_{max}, and R^2 values (*25*).

In summary, this report provides evidence that two related transcription factors, NPAS2 and Clock, may constitute intracellular redox sensors. Using test-tube reactions with purified reagents, we demonstrated that the DNA-binding activities of NPAS2 and Clock can be influenced by the redox states of NAD(H) or NADP(H). We offer three experimental observations that favor the biological validity of these observations. First, the concentration range over which reduced nicotinamide cofactors induce NPAS2 and Clock DNA-binding activity is in the low millimolar range, corresponding with the intracellular concentrations reported in the literature (*23*). Were the potency of activity either far lower (high mM) or higher (sub-mM), the activities of NPAS2 and Clock would not be capable of functioning as a redox sensor.

Second, the effects of the oxidized and reduced forms of NAD(H) and NADP(H) were shown to influence the DNA-binding activity of the NPAS2:BMAL1 heterodimer in a reciprocally opposed manner. The very subtle difference of a single hydrogen atom on the nicotinamide ring caused the reduced cofactor to activate DNA binding and the oxidized cofactor to inhibit. All reactions were carried out in the presence of high concentrations of dithiothreitol (DTT), a stronger reducing agent than either NADH or NADPH. As such, we do not believe that NAD cofactors act by redox modification of the NPAS2, Clock, or BMAL1 polypeptides but instead serve as molecular ligands. The oxidized cofactor, NADP, inhibits NPAS2:BMAL1 DNA-binding activity, but the reduced form NADPH activates. By definition, in order for the NPAS2 and Clock polypeptides to function as redox sensors, they must respond differentially to the oxidized and reduced forms of the two principal cofactors that regulate intracellular redox—NAD(H) and NADP(H).

This reciprocal effect is the basis of the third observation favoring the hypothesis that Clock:BMAL1 and NPAS2:BMAL1 serve as bona fide redox sensors, which is the steep induction and inhibition curves observed herein. A nearly quantitative molecular switch in DNA-binding activity was observed over the relatively subtle change in redox state from 60:40 to 80:20 reduced-to-oxidized ratios of NADP(H). In biochemical terms, the properties of this switch are best described by an apparent Hill coefficient of 15 (Fig. 3A). Any rendering of the Hill coefficient above a value of 1 can be interpreted to reflect elements of cooperativity. A Hill coefficient of 15 portrays an exceptionally coopera-

tive reaction. Whereas proper accounting of the biophysical and biochemical nature of this cooperativity remains to be elucidated, the reaction does offer multiple opportunities for allosteric regulation. At least two equilibria might be influenced by the redox state of NAD cofactors: (i) formation of NPAS2:BMAL1 heterodimers and (ii) reversible interaction of the NPAS2:BMAL1 heterodimer with its DNA substrate. Indeed, having observed that cofactor redox state influences both the K_d and B_{max} of the NPAS2:BMAL1 heterodimer for its DNA substrate, we speculate that this redox switch will manifest its consequences at multiple levels.

We propose that fluctuations in cellular redox can act to directly entrain the molecular clock. It is well established that changes in the abundance of reduced fuels correlate with fluctuations in cellular redox state (*29*–*31*). Cells respond to the liberal availability of reduced fuels by mobilizing metabolic pathways that convert oxidized NAD cofactors into their reduced counterparts. By contrast, such reducing equivalents are expended for the purpose of energy-dependent biosynthetic reactions during periods of starvation. For most metazoan organisms, this cycle oscillates regularly as a function of the day-night cycle. Nocturnal animals feed at night and starve by day, with diurnal animals exhibiting the opposite pattern of feeding behavior. It has been observed that RF can entrain activity rhythms in rodents (*12*, *13*) by modulation of the molecular circadian clock (*14*, *15*). We speculate that RF may entrain the molecular rhythm directly through induced change in cellular redox potential.

It is reasonable to postulate that RF, through induced alteration of intracellular redox levels, might be capable of direct entrainment of the molecular clock in peripheral tissues such as intestine or liver. RF has also been found to entrain molecular rhythms in the forebrain (*32*). Fluctuation in food energy does not translate to rhythmic oscillation in blood glucose in the principal site of expression of NPAS2—the mammalian forebrain (*26*, *33*). How then might RF reprogram a circadian oscillatory device located in the forebrain?

Although blood glucose concentrations remain constant as a function of the LD cycle, rates of glucose uptake and glycolysis are known to fluctuate as a function of neuronal activity (*34*–*36*). Indeed, differential rates of energy consumption form the basis of brain imaging techniques that use 2-deoxy-glucose as a marker (*37*, *38*). Morphological studies have shown that astrocytes form the proximal, cellular bed adjacent to the vascular system of the brain (*39*). In response to extracellular glutamate, which is plentiful in brain nuclei that are active with respect to neurotransmission, astrocytes elevate their intrinsic rate of glycolysis, resulting in the production of lactate (*34*–*36*). Astrocyte-generated lactate is released extracellularly and used as the principal energy source of neurons through a facilitated monocarboxylate transporter present in neurons (*40*–*42*). Because rates of glycolysis and lactate production oscillate as a function of neuronal activity, it is possible that the intracellular redox potential of neurons fluctuates accordingly despite homeostatic blood glucose levels in the brain. If so, neurons containing the molecular clock might be entrained by neuronal activity through fluctuations in the ratios of reduced-to-oxidized NAD cofactors. This speculation is supported by our finding that LDHA is a direct target of NPAS2:BMAL1 (Fig. 1). It has likewise been reported that expression of the gene encoding the neuron-specific lactate transporter, MCT2, also oscillates as a function of the LD cycle (*43*). If both the import and metabolism of lactate are under diurnal control, neuronal redox levels should fluctuate in a manner concordant with both brain activity and the LD cycle. Indeed, preliminary observations suggest that lactate administration potentiates NPAS2/BMAL activity in cultured neuroblastoma cells (*44*).

This view of entrainment can best be evaluated in the context of the pathway by which light entrains circadian rhythm in the SCN. Light perceived by the retina triggers activation of a series of neuronal connections coalescing at the SCN (*11*). In vivo measurements show that SCN electrical activity is rhythmic, with peak activity during the light phase of a LD cycle (*45*, *46*). If the hypothesis put forward herein is tenable, one could logically predict that interplay between neurons and astrocytes might form an interlocked loop wherein glucose uptake, glycolysis, and lactate production by astrocytes would be regulated by neuronal activity (*47*). Likewise, rhythmic astrocyte-derived production of lactate, as well as its uptake and metabolism by neurons, might lead to balanced oscillation of intracellular redox potential, thereby executing biochemical entrainment of the molecular clock.

Finally, as described in the accompanying report (*4*), we believe that NPAS2 functions as a positive component of a molecular clock in the mammalian forebrain, equivalent to the function of Clock in the SCN. The principal sites of NPAS2 expression include the somatosensory cortex, visual cortex, auditory cortex, olfactory tubercles, striatum, and accumbens nucleus (*48*). These regions of the forebrain process sensory information, including touch, pain, temperature, vision, hearing, and smell, as well as emotive behaviors such as fear and anxiety. We hypothesize that during wakeful-

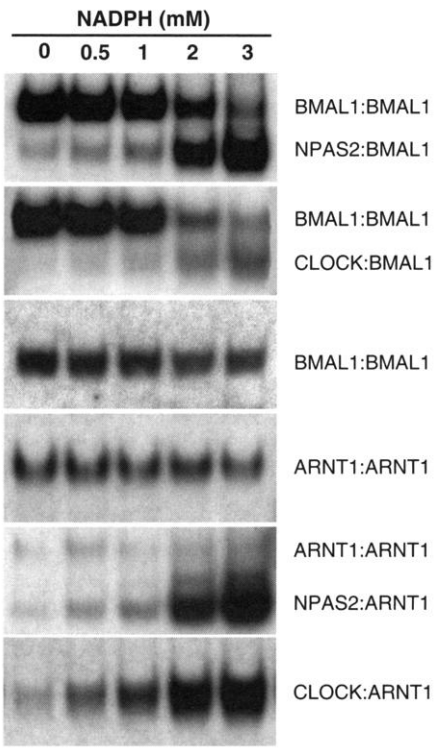

Fig. 5. Regulation by NADPH is specific to NPAS2- or Clock-containing heterodimers. Individual panels show the response of specific protein combinations to increasing amounts of NADPH. The protein combinations and corresponding DNA-bound species are indicated on the right. In all cases bHLH-PAS–containing fragments were used under standard reaction conditions (*21*, *22*).

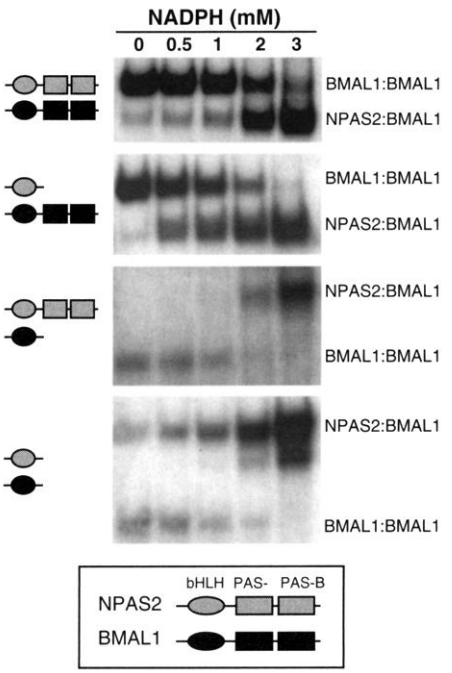

Fig. 6. The bHLH region of NPAS2 is sufficient for regulation by NADPH. Each panel shows the response of specific NPAS2 and BMAL1 fragment combinations to increasing amounts of NADPH. The various protein fragments (*21*) are shown diagrammatically on the left with NPAS2 designated in gray and BMAL1 in black. The identities of specific DNA-bound homodimeric and heterodimeric complexes are indicated on the right.

ness, these NPAS2-expressing regions of the brain receive and process stimulatory neuronal activity that entrains the molecular clock in the same manner argued for the retino-SCN pathway (*16*). This entrainment could occur by three interlinked events: (i) generation of extracellular glutamate by active neurotransmission, (ii) stimulation of glycolysis and lactate production by localized glutamate uptake into astrocytes, and (iii) fluctuation of intracellular redox potential by facilitated lactate transport and its consumption as a metabolic fuel in nearby neurons. If correct, this hypothesis may ultimately help to explain how the mammalian forebrain oscillates between states of alertness and tiredness.

References and Notes

1. R. J. Konopka, S. Benzer, *Proc. Natl. Acad. Sci. U.S.A.* **68**, 2112 (1971).
2. J. C. Dunlap, *Cell* **96**, 271 (1999).
3. N. Gekakis *et al.*, *Science* **280**, 1564 (1998).
4. M. Reick, J. A. Garcia, C. Dudley, S. L. McKnight, *Science* **293**, 506 (2001).
5. J. B. Hogenesch, Y. Z. Gu, S. Jain, C. A. Bradfield, *Proc. Natl. Acad. Sci. U.S.A.* **95**, 5474 (1998).
6. E. A. Griffin Jr., D. Staknis, C. J. Weitz, *Science* **286**, 768 (1999).
7. K. Kume *et al.*, *Cell* **98**, 193 (1999).
8. H. Abe *et al.*, *Neurosci. Lett.* **258**, 93 (1998).
9. C. S. Pittendrigh, *Annu. Rev. Physiol.* **55**, 16 (1993).
10. J. S. Takahashi, *Annu. Rev. Neurosci.* **18**, 531 (1995).
11. R. Y. Moore, *Ciba Found. Symp.* **183**, 88 (1995).
12. F. K. Stephan, J. M. Swann, C. L. Sisk, *Behav. Neural Biol.* **25**, 545 (1979).
13. R. E. Mistlberger, *Neurosci. Biobehav. Rev.* **18**, 171 (1994).
14. F. Damiola *et al.*, *Genes Dev.* **14**, 2950 (2000).
15. K. A. Stokkan *et al.*, *Science* **291**, 490 (2001).
16. H. Wakamatsu *et al.*, *Eur. J. Neurosci.* **13**, 1190 (2001).
17. For Northern blots (*26*), we prepared a G3PDH probe by reverse transcription polymerase chain reaction (RT-PCR) using mouse brain RNA as a template and the following primers: forward, 5′-ACCACAGTCCATGCCATCAC-3′; reverse, 5′-TCCACCACCCTGTTGCTGTA-3′. The resulting PCR product was cloned into pGEM-T and confirmed by DNA sequence analysis. A partial cDNA clone corresponding to bases 293 to 899 of the LDHA gene (GenBank, accession number BC001829) was used as the probe for LDHA mRNA.
18. GenBank accession Y00309 provided genomic sequence information for the mouse LDHA gene. A ~1.5-kb fragment of the mouse LDHA gene promoter and upstream sequences was amplified with the following primers: forward, 5′-GGAGCTCCCCTGTCCACGAATCCTTCTGG-3′; reverse, 5′-AGATCTGGCCTTAAATGGAAGCTCCGCGC-3′. The PCR product was cloned into the Sac I and Bgl II sites of the pGL3-Basic luciferase reporter plasmid.
19. GenBank accession Y00309 revealed the location of the TATA box of the LDHA gene promoter at nucleotides −20 to −25 relative to the transcription start site. The sequence also contained optimal NPAS2:BMAL1 binding sites at nucleotides −78 to −83 (sequence 5′-CACGTG-3′) and −171 to −176 (sequence 5′-CACGTG-3′).
20. G. Kopperschlager, J. Kirchberger, *J. Chromatogr. B Biomed. Appl.* **684**, 25 (1996).
21. The genes encoding mouse (m) NPAS2 bHLH-PAS (1–416), mNPAS2 bHLH (1–116), and mClock bHLH-PAS (1–342) were cloned into the vector pHISTEV and expressed in the BL-21(DE3) strain of *Escherichia coli*. The proteins were purified from inclusion bodies with Ni-NTA agarose (Qiagen, Valencia, CA), dialyzed into buffer A [25 mM Hepes (pH 7.5), 50 mM NaCl, 1 mM EDTA, and 1 mM DTT] supplemented with 20% glycerol, and frozen at −80°C. The gene encoding human (h) BMAL1 bHLH-PAS (1–447) was cloned into the pParallel-MBP vector (*49*), expressed in *E. coli*, and purified with amylose resin. hARNT1 bHLH-PAS (1–506) was expressed in Sf-9 cells with a recombinant baculovirus based on the BAC-to-BAC system (Gibco BRL) and purified with Ni-NTA agarose. The hBMAL1 bHLH (75–126) peptide was prepared by solid-phase peptide synthesis and purified by standard high-performance liquid chromatography methods.
22. For EMS assays (*50*), reactions contained recombinant transcription factors (0.3 to 0.5 μg/reaction or, in the case of the bHLH fragments, 100 ng/reaction) and radioactive, double-stranded oligonucleotide probe (200 nM). The sequence of the two strands of the DNA probe were 5′-GGGGCGCCACGTGAGAGG-3′ and 5′-GGCCTCTCACGTGGCGCC-3′. The DNA was radiolabeled by filling in with [α-^{32}P]deoxycytidine triphosphate with the Klenow fragment of DNA polymerase. Solutions of nicotinamide dinucleotides, prepared fresh for each experiment, were solubilized in deionized water, and concentrations were determined by absorbance at 260 nm. For the NAD cofactor response, the binding data were fit with nonlinear regression to variable slope sigmoidal dose-response curves with the PRISM program (GraphPad, San Diego, CA).
23. H. U. Bergmeyer, *Methods of Enzymatic Analysis* (Academic Press, New York, ed. 2, 1974), vol. 4.
24. J. Rutter, M. Reick, L. C. Wu, S. L. McKnight, data not shown.
25. Saturation-binding assays were carried out as described for conventional EMS assays (*22*) with final double-stranded oligonucleotide concentrations ranging from 2.4 to 800 nM. Saturation data were fit with nonlinear regression to a single-site saturation curve with the PRISM program.
26. Y. D. Zhou *et al.*, *Proc. Natl. Acad. Sci. U.S.A.* **94**, 713 (1997).
27. D. P. King *et al.*, *Cell* **89**, 641 (1997).
28. A discussion of the bHLH of NPAS2 as a sensor of nicotinamide nucleotides is available as supplementary information on *Science* Online (*51*).
29. R. L. Veech *et al.*, *Biochem. J.* **115**, 609 (1969).
30. D. H. Williamson, P. Lund, H. A. Krebs, *Biochem. J.* **103**, 514 (1967).
31. O. Garofalo, D. W. Cox, H. S. Bachelard, *J. Neurochem.* **51**, 172 (1988).
32. M. Reick, S. L. McKnight, unpublished data.
33. J. E. Gerich, *Diabetes Obes. Metab.* **2**, 345 (2000).
34. L. Pellerin, P. J. Magistretti, *Proc. Natl. Acad. Sci. U.S.A.* **91**, 10625 (1994).
35. ———, *Dev. Neurosci.* **18**, 336 (1996).
36. S. Takahashi, B. F. Driscoll, M. J. Law, L. Sokoloff, *Proc. Natl. Acad. Sci. U.S.A.* **92**, 4616 (1995).
37. M. E. Phelps *et al.*, *Ann. Neurol.* **6**, 371 (1979).
38. L. Sokoloff *et al.*, *J. Neurochem.* **28**, 897 (1977).
39. A. Peters, S. L. Palay, H. F. Webster, *The Fine Structure of the Nervous System: Neurons and Their Supporting Cells* (Saunders, Philadelphia, PA, 1991).
40. L. Pellerin, G. Pellegri, J. L. Martin, P. J. Magistretti, *Proc. Natl. Acad. Sci. U.S.A.* **95**, 3990 (1998).
41. A. Schurr *et al.*, *Science* **240**, 1326 (1988).
42. A. Schurr *et al.*, *J. Neurosci.* **19**, 34 (1999).
43. P. J. Magistretti, personal communication.
44. Supplementary data are available on *Science* Online (*51*).
45. S. T. Inouye, H. Kawamura, *Proc. Natl. Acad. Sci. U.S.A.* **76**, 5962 (1979).
46. S. Yamazaki, M. C. Kerbeshian, C. G. Hocker, G. D. Block, M. Menaker, *J. Neurosci.* **18**, 10709 (1998).
47. W. J. Schwartz, H. Gainer, *Science* **197**, 1089 (1977).
48. J. A. Garcia *et al.*, *Science* **288**, 2226 (2000).
49. P. Sheffield *et al.*, *Protein Expr. Purif.* **15**, 34 (1999).
50. Z. Cao *et al.*, *Genes Dev.* **5**, 1538 (1991).
51. Supplementary data are available on *Science* Online at www.sciencemag.org/cgi/content/full/1060698/DC1.

52. We thank N. Grichine for assistance with protein structure analysis; J. Albanesi for help in analysis of equilibrium binding data; J. D. McGarry, K. Uyeda, D. Lane, and R. Estabrook for advice on the biochemistry of NAD redox; R. Bruick and J. Garcia for helpful discussions; L. Huang for synthesis of the BMAL1 bHLH-alone peptide; M. A. Phillips for pHisTev; and M. Brown and J. Goldstein for critical review of the manuscript. J.R. was supported by an NIH predoctoral fellowship (NIH5-T32-GM08-291-12) and S.L.M. by NIH grant 1RO1MH59388 and unrestricted funds provided by an anonymous donor.

14 March 2001; accepted 11 June 2001
Published online 5 July 2001;
10.1126/science.1060698
Include this information when citing this paper.

Absence of Junctional Glutamate Receptor Clusters in *Drosophila* Mutants Lacking Spontaneous Transmitter Release

Minoru Saitoe,[1,2]* Thomas L. Schwarz,[3]† Joy A. Umbach,[4] Cameron B. Gundersen,[4] Yoshiaki Kidokoro[1]

Little is known about the functional significance of spontaneous miniature synaptic potentials, which are the result of vesicular exocytosis at nerve terminals. Here, by using *Drosophila* mutants with specific defects in presynaptic function, we found that glutamate receptors clustered normally at neuromuscular junctions of mutants that retained spontaneous transmitter secretion but had lost the ability to release transmitter in response to action potentials. In contrast, receptor clustering was defective in mutants in which both spontaneous and evoked vesicle exocytosis were absent. Thus, spontaneous vesicle exocytosis appears to be tightly linked to the clustering of glutamate receptors during development.

In 1952, Fatt and Katz described miniature end-plate potentials, which provided a basis for the theory of quantal synaptic transmission (*1*). A single miniature end-plate potential arises when a synaptic vesicle fuses spontaneously with the presynaptic membrane and releases a quantum of transmitter (spontaneous vesicle exocytosis). However, little is known about the